4.5.4 Dent Type *G* Stress Behavior

Unrestrained longitudinal Type G dents exhibit *long* dent behavior like *Type* A dents. This dent type was not tested experimentally. The general failure mode found for longitudinal Type G dents is Mode 1. The increased dent length as compared to Type A dents causes more rebound of the longer Type G dents. This will make larger diameter pipes with Type G dents susceptible to Mode 1 failures that exhibited Mode 2 failures with Type A dents.

Bending stress causes high outside surface transverse stress in the dent contact region of Type G dents. The outside surface transverse stress distribution during pressure cycling for a 10 percent *d/D* Type G dent in Pipe 18-3 is given in Fig. 4-89. The entire contact region has a high stress range. At a distance of 24 in. from the center of the dent, the stress values are near the values of the membrane hoop stress. This length of pipe with the stress affected by the dent is longer than the length of the shorter Type A dents. From Fig. 4-66, the affected length for a Type A dent is about 18 in. from the center of the dent. The affected length are similar for the two dent types if the measurement is taken from the end of dent contact.

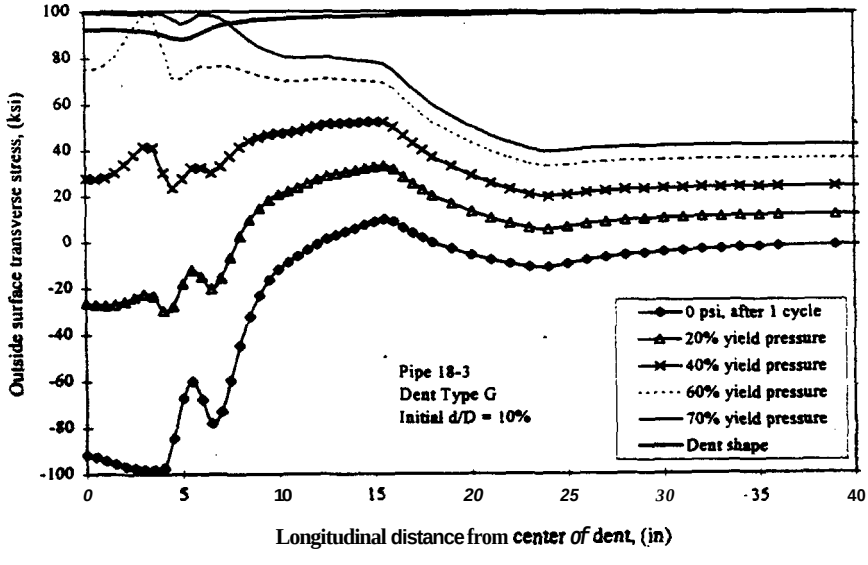

Figure 4-89: Outside surface transverse stress behavior during pressure cycling for Pipe 18-3 with a 10 percent *d/D* Type G dent.

Outside surface transverse stress contour plots are given for the **10** percent *d/D* Type G dent in Pipe **18-3** in Figs. **4-90** and **4-91** at zero pressure and at the design pressure. The contour plots are similar to the plots for the Type **A** dents given in Figs. **4-67** and **4-68.** The only difference in the stress behavior between the two dent types is the length of pipe affected which is directly related to the dent length.

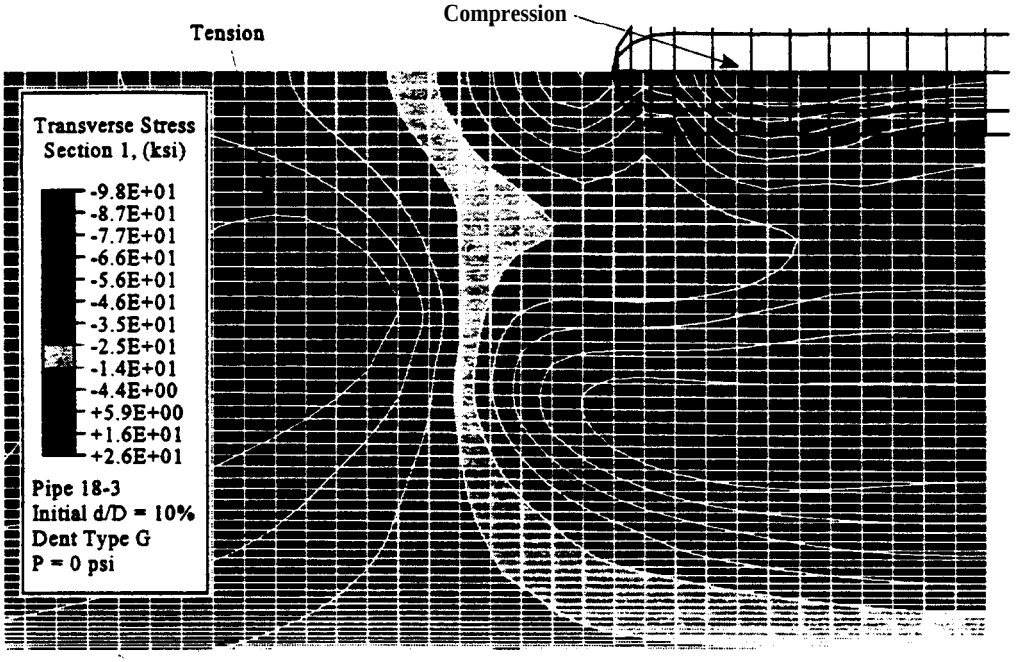

Figure **4-90:** Outside surface transverse stress contour plot for Pipe **18-3** with a **10** percent *d/D* Type G dent at 0 psi.

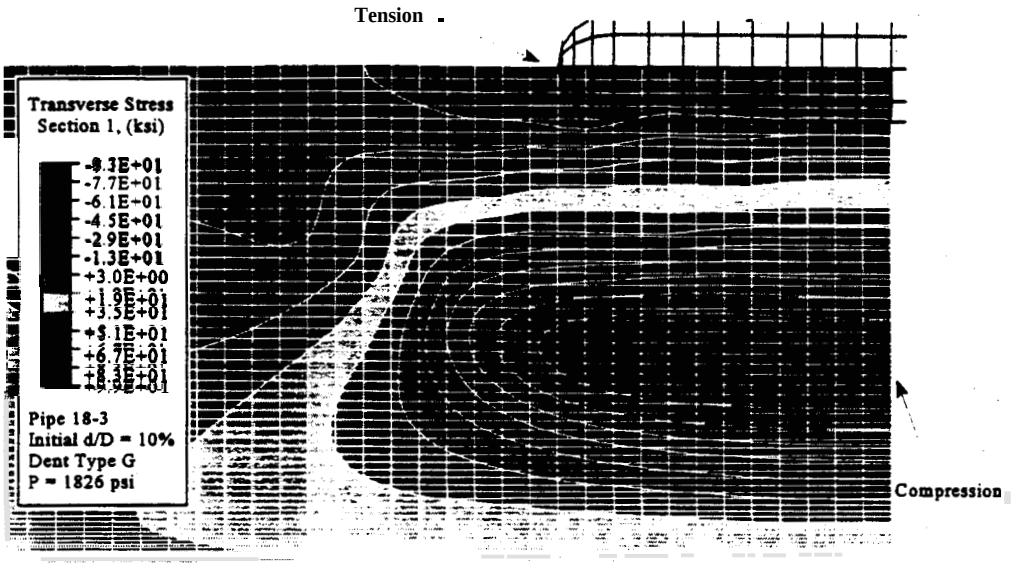

Figure **4-91:** Outside surface transverse stress contour plot for Pipe 18-3 with a 10 percent *d/D* Type G dent at the design pressure.

For the Type **A** dents, the mode of failure is influenced by diameter, thickness, and dent depth. The failure mode of Type G dents is similar, except that the transition of failure mode occurs at larger diameters **as** compared to Type A dents. The outside surface transverse **stress** of a 10 percent *d/D* Type G dent in Pipe 30-3 is **given** in Fig. **4-92. This** dent will be susceptible to Mode 1 failures. The largest **stress** range is located at the center of the dent. The dent periphery **also has a** high stress range, **but** not **as** high **as** the **stress** range in the center of the dent. The stress in the periphery can be considered **as** part of the Mode 1 **stress** distribution. The reduction of stress range **between** the center of the contact region and periphery is caused by the stiffness surrounding the ends of the contact region. The two ends can be thought of **as** two short dents with close proximity. Short dents such **as** Type BH dents have contact regions with low stress ranges similar to the stress range of the ends of the Type G dent.

Comparison of Fig. **4-92** with a Type G dent and Fig. **4-74** with a Type **A** dent in Pipe

30-3 show that transition of failure mode occurs at smaller diameters for the shorter Type A dents. The Type A dent has a higher stress range in the periphery of the dent as compared to the contact region.

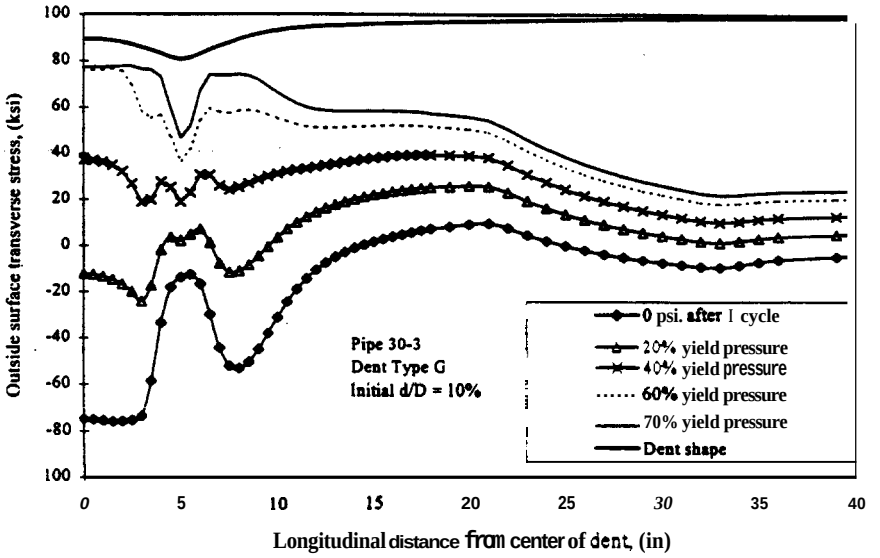

Figure 4-92: Outside surface transverse stress behavior during pressure cycling for Pipe 30-3 with a 10 percent *d/D* Type G dent.

Failure Mode 2 for Type G dents only occurs in deep dents of very large pipes. The transverse stress distribution for a 10 percent *d/D* Type G dent in Pipe 48-6 is given in Fig. 4-93. The stress ranges in the contact region and in the dent periphery are identical for this given pipe size and dent depth. Due to the contact damage found in the contact region, this dent will have a Mode 1 failure. Increasing the dent depth shifts the mode of failure. The stress distribution for a 15 percent *d/D* Type G dent in Pipe 48-6 is given in Fig. 4-94. The increase in dent depth causes a decrease in the *stress* range of the contact region. This dent will likely have failure Mode 2 with peripheral fatigue crack development.

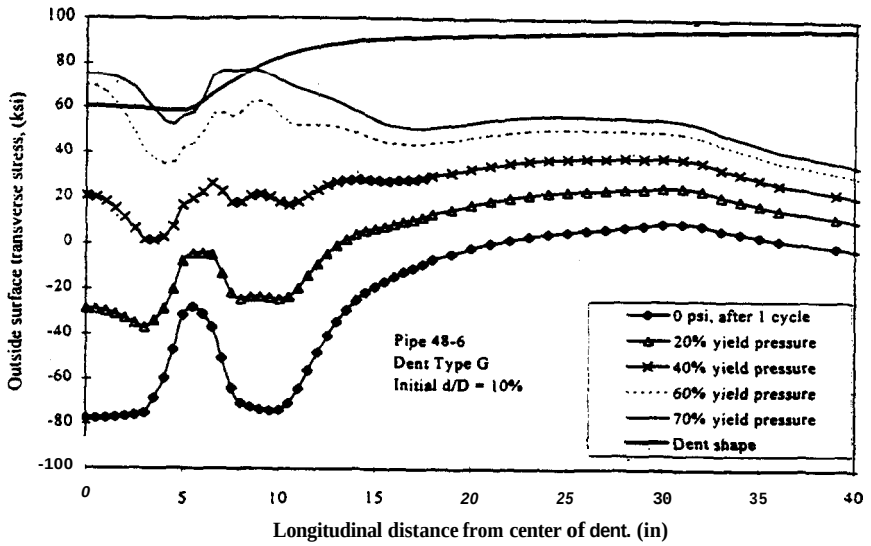

Figure 4-93: Outside surface transverse stress behavior during pressure cycling for **Pipe 48-6 with a 10 percent *d/D*** Type **G dent.**

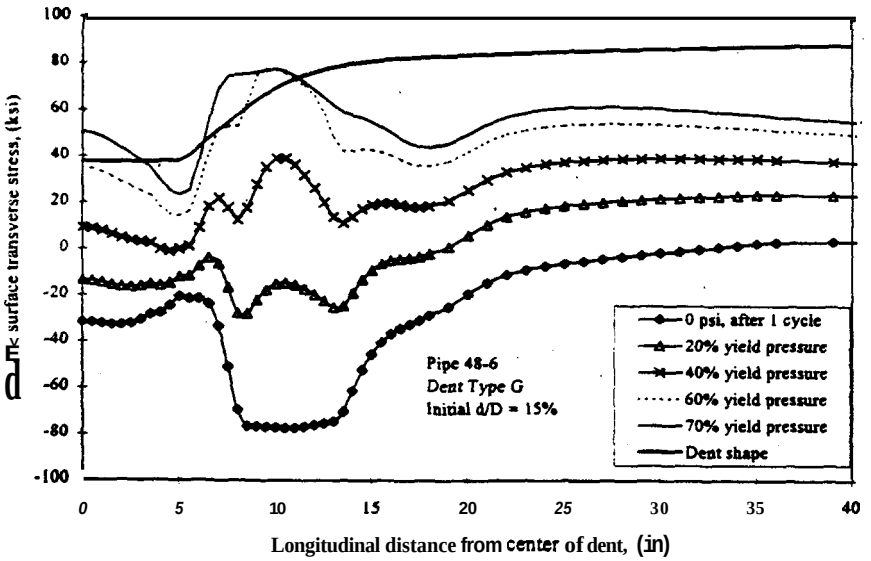

Figure 4-94: Outside surface transverse stress behavior during pressure cycling for Pipe 48-6 with **a 10 percent *d/D*** Type **G dent.**

For the broad range of parameters modeled for Type G dents, the fatigue behavior remains the same with Mode 1 failures. Mode 2 failures only occur in very large pipes with deep dents. This will be irrelevant in terms of acceptance criteria since all shallow Type G dents exhibit Mode 1 failure regardless of the pipe dimensions. Table 4-13 shows the predicted failure modes of the unrestrained Type G dents modeled.

Table 4-13: Dent Type G Predicted Failure Modes.

Diameter (in)	Thickness (in)	Initial d/D (%)				
		5	7.5	10	12.5	15
12	0.250	1	1	1	1	1, 2
12	0.375	1	1	1	1	1, 2
12	0.500	1	1	1	1	1, 2
18	0.250	1	1	1	1	1, 2
18	0.375	1	1	1	1	1, 2
18	0.500	1	1	1	1	1, 2
24	0.250	1	1	1	1, 2	1, 2
24	0.375	1	1	1	1, 2	1, 2
24	0.500	1	1	1	1, 2	1, 2
24	0.625	1	1	1	1	1, 2
30	0.250	1	1	1	1, 2	1, 2
30	0.375	1	1	1	1	1, 2
30	0.500	1	1	1	1	1, 2
30	0.625	1	1	1	1	1, 2
30	0.750	1	1	1	1, 2	1, 2
36	0.250	1	1	1, 2	1, 2	1, 2
36	0.375	1	1	1	1, 2	1, 2
36	0.500	1	1	1	1, 2	1, 2
36	0.625	1	1	1	1, 2	1, 2
36	0.750	1	1	1, 2	1, 2	2, 1
48	0.375	1	1	1	1, 2	1, 2
48	0.500	1	1	1	1, 2	1, 2
48	0.625	1	1	1	1, 2	2, 1
48	0.750	1	1	1, 2	2, 1	2

Modes 1 and 2 represent long and short dent behavior, respectively.
If both are given, the most probable mode of failure is listed first.

4.5.5 Dent Type H Stress Behavior

Type H dents behave as long dents with stress distributions indicative of failure Mode 1. An example transverse stress distribution is given in Fig. 4-95 for a 10 percent *d/D* Type H dent in Pipe 18-3. The transition of Type H dents from Mode 1 to Mode 2 failures occurs at smaller pipe sizes as compared to Type G dents due to the decreased length of the contact region. The width of the Type H indenter does not change the behavior as compared to the thinner indenter Types A and G. Table 5.14 shows the predicted failure modes of the unrestrained Type H dents modeled.

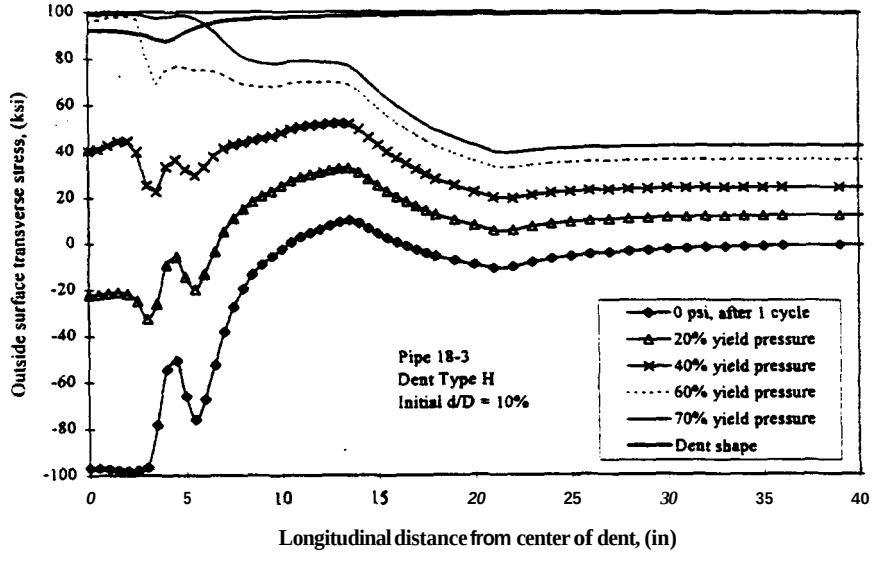

Figure 4-95: Outside surface transverse stress behavior during pressure cycling for Pipe 18-3 with a 10 percent *d/D* Type H dent.

Table 4-14: Dent Type H predicted failure modes.

Diameter (in)	Thickness (in)	Initial d/D (%)				
		5	7.5	10	12.5	15
18	0.250	1	1	1	1, 2	1, 2
18	0.375	1	1	1	1, 2	1, 2
18	0.500	1	1	1	1	1, 2
48	0.375	1	1	1	1	1
48	0.500	1	1	1, 2	1, 2	2, 1
48	0.625	1	1, 2	2, 1	2	2
48	0.750	1	1, 2	2, 1	2	2

Modes 1 and 2 represent long and short dent behavior, respectively.
If both are given, the most probable mode of failure is listed first.

4.6 BEHAVIOR OF UNRESTRAINED TRANSVERSE, SPHERICAL, AND PLATE DENTS

4.6.1 Transverse Dents

Transverse dents were modeled for Type A and G indenters (see Fig. 4-1). Transverse dents are labeled as Type A-T and G-T where T represents the transverse dent orientation. The rebound and stress behavior of transverse dents was studied to provide comparisons with longitudinal dents. Model plots of indentation, initial rebound, and final rebound are given in Fig. 4-96 for Pipe 18-3 with a 10 percent d/D Type G-T dent.

The change in orientation adds an additional parameter that may affect rebound and stress behavior. For longitudinal dents, the entire length of the indenter has contact with the pipe wall. With transverse dents, the entire length of the indenter may not be in contact. At the start of indentation, contact initiates at the center of the indenter. Increasing the dent depth increases the contact length as the pipe deforms to the shape of the indenter. The full length of the indenter may or may not have contact. This is influenced by dent depth, pipe diameter, and indenter length. For longitudinal dents, the transfer of the indenter force to the pipe concentrated at the ends of the indenter. The transfer of the indenter force for transverse dents will be different, especially if the ends of the indenter do not have contact.

The cross section displacements during indentation of Type A-T dents are given in Fig. 4-97 for Pipe 18-3. At a dent depth of 5 percent d/D, the end of the Type A-T indenter is not in contact with the pipe. An increase in dent depth to 7.5 percent d/D puts the full length of the indenter (6.0 in.) in contact. The circular shape of the pipe deforms to the straight shape of the rigid indenter. As the dent depth increases, the curvature outside the end of the indenter increases after the full indenter length is in contact. For dents with the entire indenter length in contact, the most severe contact damage will be located at the ends of the indenter similar to that of all longitudinal dents. For dents without the entire indenter length in contact, the contact damage will be more uniform throughout the contact region.

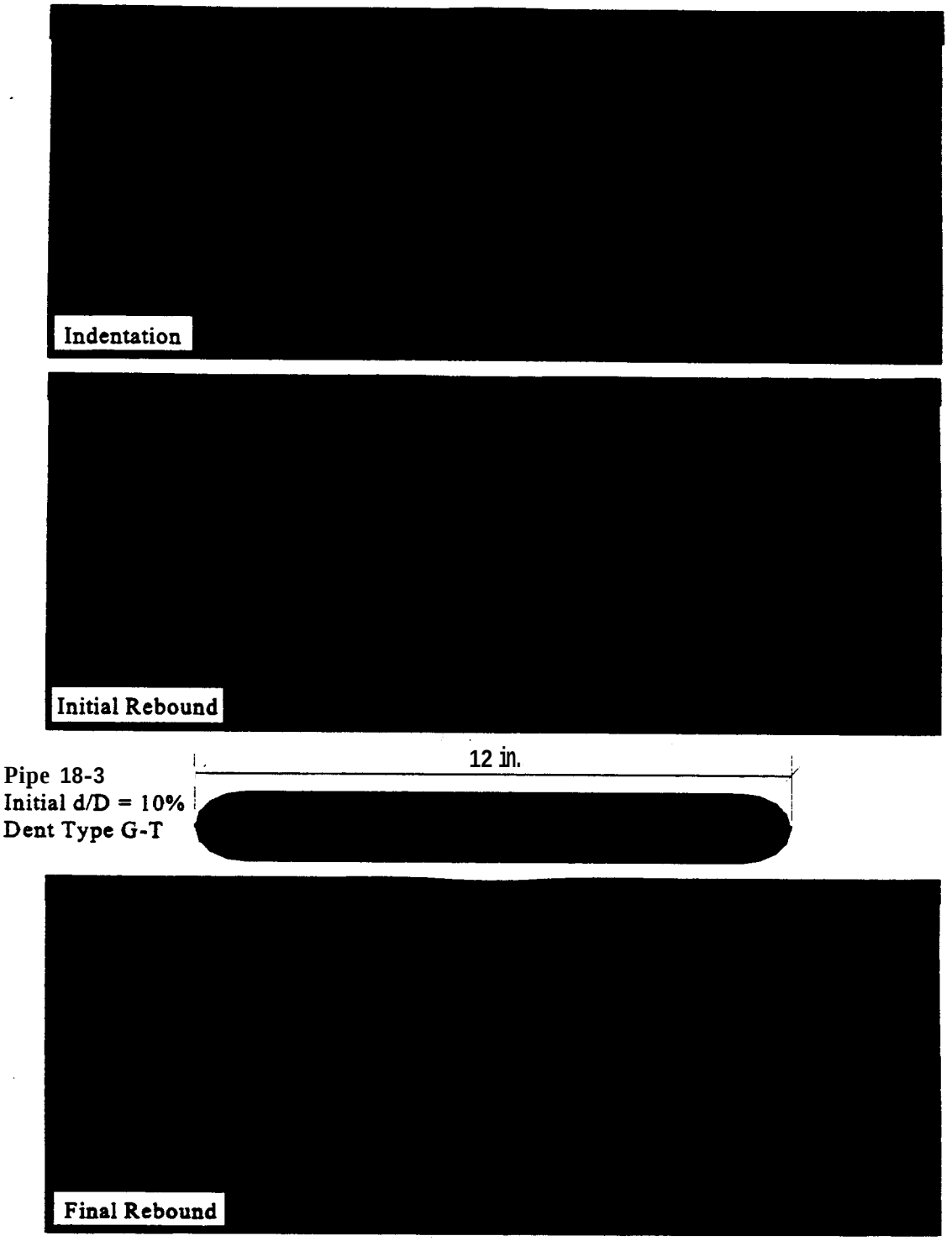

Figure 4-96: Dent Type G-T model plots of indentation, initial rebound, and final rebound.

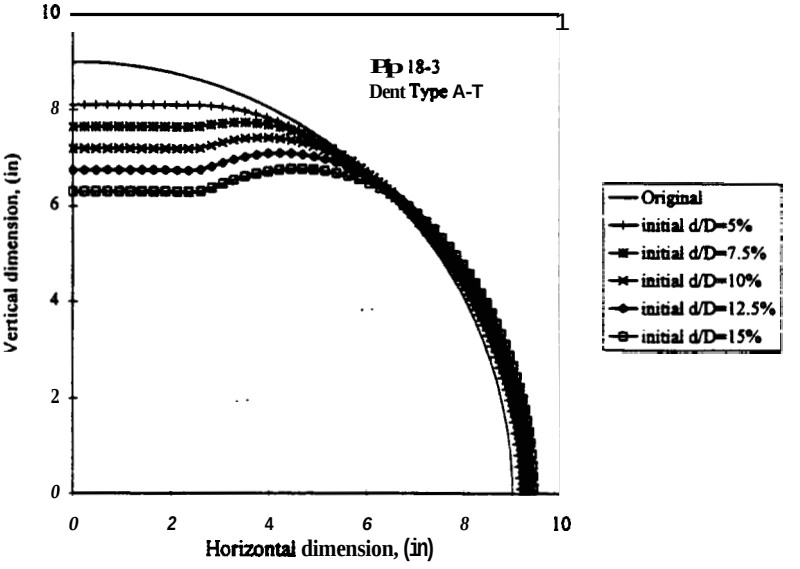

Figure 4-97: Dent Type A-T displaced cross section at indentation for Pipe 18-3.

An increase in indenter length changes the contact length of transverse dents. The cross section displacement during indentation of Type G-T dents are given in Fig. 4-98. For the Type G-T indenter, the ends of the indenter do not have contact with the pipe surface until a depth of approximately 12.5 percent *d/D* as compared to 5 percent *d/D* for the Type A-T indenter. Less contact damage occurs at the ends of the indenter for the Type G-T indenter as compared to the Type A-T indenter. The curvature near the end of the Type G-T dents is much less severe as compared to Type A-T dents due to the increased dent length. The curvature around the ends of transverse indenters increases the localized stiffness at the end of the contact region as with longitudinal dents. Since a higher degree of curvature surrounds the shorter Type A-T dents, they will have less rebound at compared to the longer Type G-T dents.

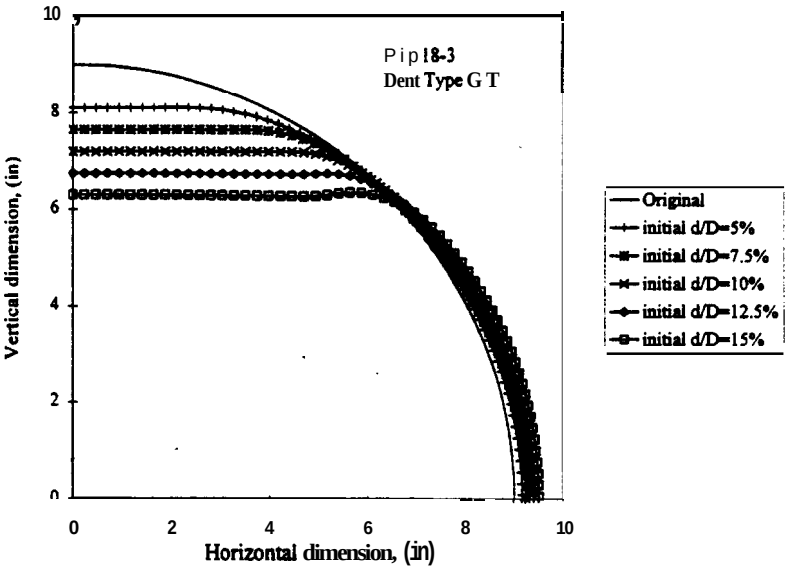

Figure 4-98: Dent Type G-T displaced cross section at indentation for Pipe 18-3.

The shapes of the Types A-T and G-T dents after initial and final rebound for Pipe 18-3 are given in Figs. 4-99 and 4-100. The Type A-T dents have the characteristic bulge found in longitudinal dents with long dent behavior though oriented in the perpendicular direction. The dent length does not influence the rebound behavior as in longitudinal dents. Transverse dents rebound towards the circular shape of the cross section, thus changing the initial flat shape of the dent to a final shape that is curved like the circular cross section. The stiffness at the ends of the contact region fiom the surrounding curvature make that local area experience less rebound which causes the rebounded dent shape to *appear* bulged. The Type G-T dents do not show the bulge due to the decrease in stiffness of the ends of the contact region from the increased dent length as compared to the shorter Type A-T dent length.

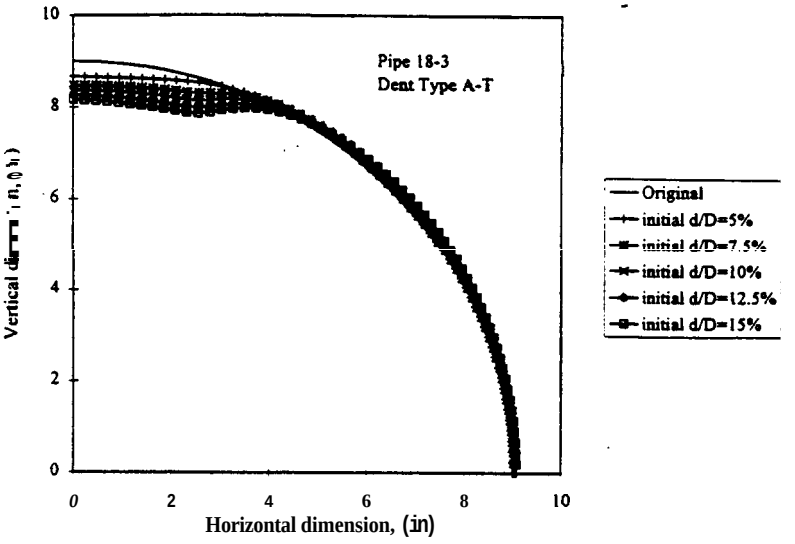

Figure 4-99: Dent Type **A-T displaced cross section after** fmal **rebound for Pipe 18-3.**

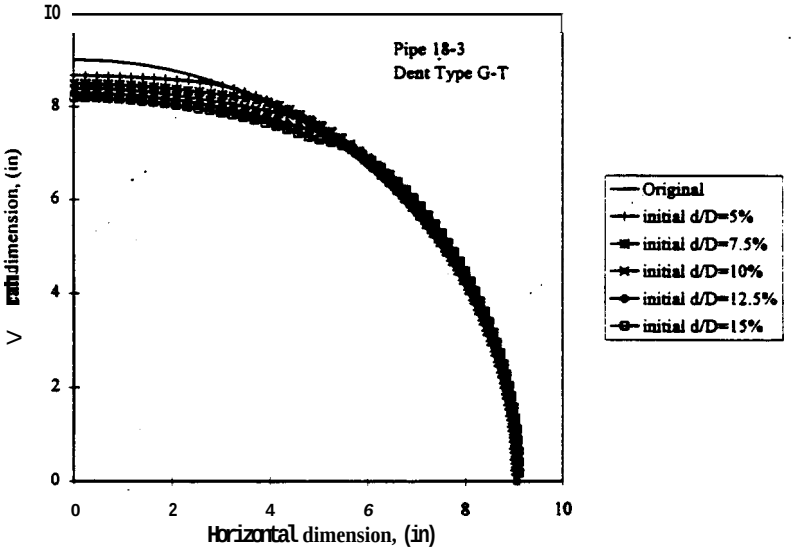

Figure 4-100: Dent Type G-T **displaced cross section** after **final rebound for Pipe 18-3.**

The rebound characteristics of transverse dents is influenced by diameter, thickness, and dent type. An increase in diameter causes an increase in rebound based on *d/D*. An increase in thickness causes a decrease in rebound. Longer dents will have more rebound than shorter dents. The dent depth measurements used are based on the maximum dent depth found in the contact region. For the **5** percent ***d/D*** Type **A-T** dent shown in Fig. 4-99, the maximum depth will be located at the center of the dent contact region, whereas it will be located at the end of the dent contact region for the **15** percent ***d/D*** Type **A-T** dent. The depth measurements were based on the shortest **radius** to the center of the pipe cross section.

A graph of final dent depth (*d/D*) vs initial dent depth (*d/D*) for transverse dents of **Type A-T** and G-T for 18 in. diameter pipes is given in Fig. 4-101. Both dent types have similar rebound characteristics except for the deeper dent depths in Pipe 18-4. The shallow dents for both dent **types** are similar since the contact region is identical regardless of indenter length since the ends of the indenters are not in contact. The contact length changes **between** the dent **types** with increasing dent depth causing dents of shorter length to have less rebound.

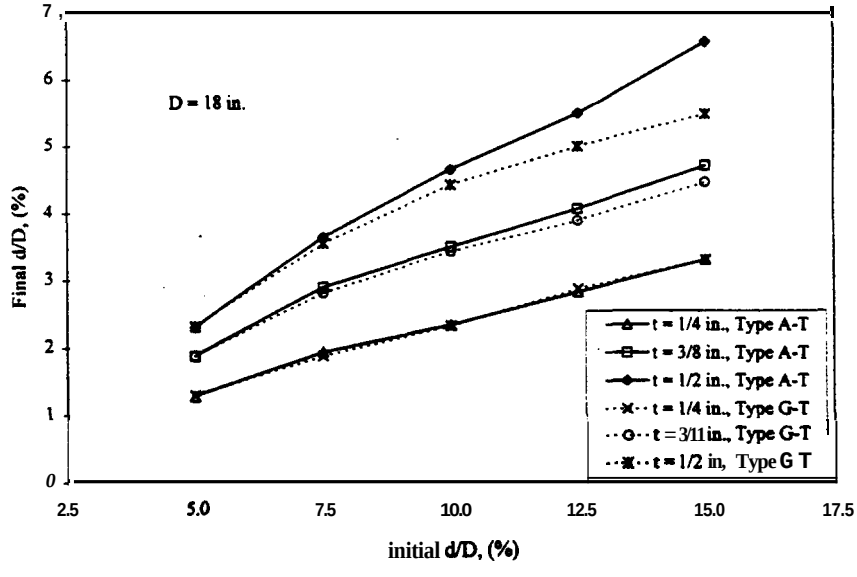

Figure 4-101: Final dent depth (*d/D*) vs. **initial** dent depth (*d/D*) for dent **Types A-T** and G-T in 12 in. pipes.

The Rebound Ratio found for longitudinal dents is applicable to transverse dents. The increase of contact length with increasing dent depth causes the Rebound Ratio to not be a constant with respect to dent depth, but the Rebound Ratio can be assumed constant without significant error. Figs. 4-102 and 4-103 give plots of Rebound Ratio vs initial dent depth for transverse dents in 18 in. and 48 in. pipes, respectively.

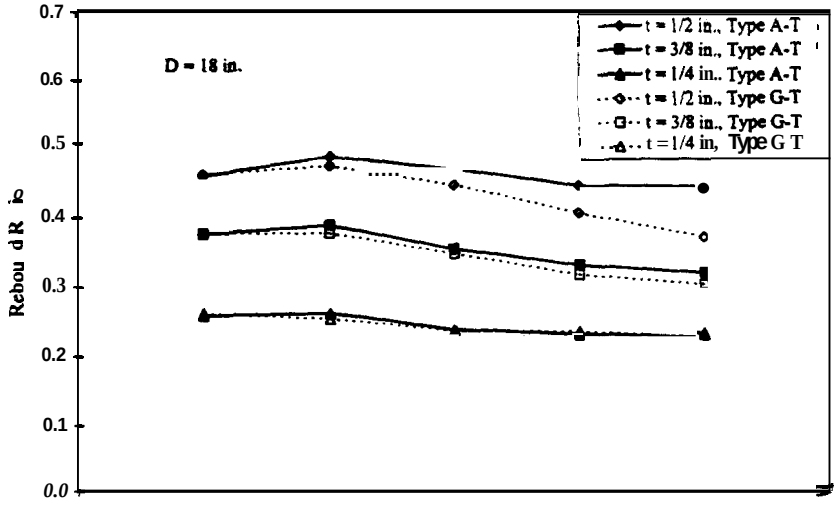

Figure 4-102: Rebound Ratio vs. initial dent depth for transverse dents in 18 in. Pipes.

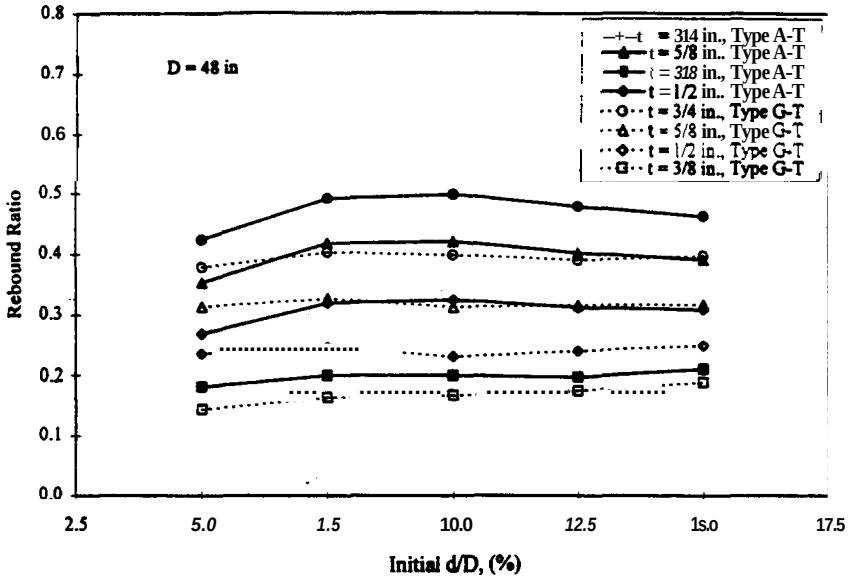

Figure 4-103: Rebound Ratio vs. initial dent depth for transverse dents in 48 in. Pipes.

For the *smaller* diameter pipe, the Rebound Ratio decreases with increasing dent depth, especially for the Type G-T dents. The Rebound Ratio remains constant for both dent types in the larger diameter pipe. The ratios *are* near constant and will be averaged as with the longitudinal dents resulting is Table 4-15.

Table 4-15: Rebound Ratio for Transverse Dents.

Thickness, t (in.)	Diameter, D (in.)			
	18		24	
	A-T	G-T	A-T	G-T
0.250	0.24	0.24	-----	-----
0.375	0.35	0.34	0.20	0.17
0.500	*0.46*	0.43	0.31	0.24
0.625	-----	-----	0.40	0.32
0.750	-----	-----	0.47	0.39

Longitudinal and transverse dent have comparable rebound characteristics. The values given for Rebound Ratio in Table 4-15 for transverse dents are similar to corresponding values in Tables 4-7 and 4-9 for longitudinal dent Types A and G.

The stress behavior of transverse dents was not studied as extensively as longitudinal dents. As with the transverse dents, stress data was only recorded along node set TOP. No experimental testing has been performed on transverse Type A-T or G-T dents. Fatigue-failure locations may or may not be located along node set TOP for *transverse* dents. The recorded stress data and contour plots show locations of possible fatigue failure.

The most probable fatigue failure mode is assumed to involve longitudinal fatigue cracks developing in the contact region or periphery of node set TOP. The outside surface transverse stress distribution for a 10 percent *d/D* Type A-T Dent in Pipe 18-3 is given in Fig. 4-104. The highest stress range is located in the dent periphery. The contact region has a slightly lower stress range, but is at a location of contact *damage* unlike the dent periphery. Thus, fatigue failures could occur in either the contact or periphery of the dent. All Type A-T and G-T dents modeled in 18 in. diameter pipes have *stress* distributions similar to that given in Fig. 4-104.

Contour plots of the outside surface transverse *stress* for a 10 percent *d/D* Type G-T dent at 0 psi and the design pressure are given in Figs. 4-105 and 4-106, respectively. At 0 psi, the center of the contact region and the periphery are in a *stress* state of compression. At the design pressure, these regions *are* in a transverse *stress* state of high tension. The ends of the contact region remain in compression throughout pressure cycling. Thus, longitudinal fatigue cracks would develop along node set TOP.

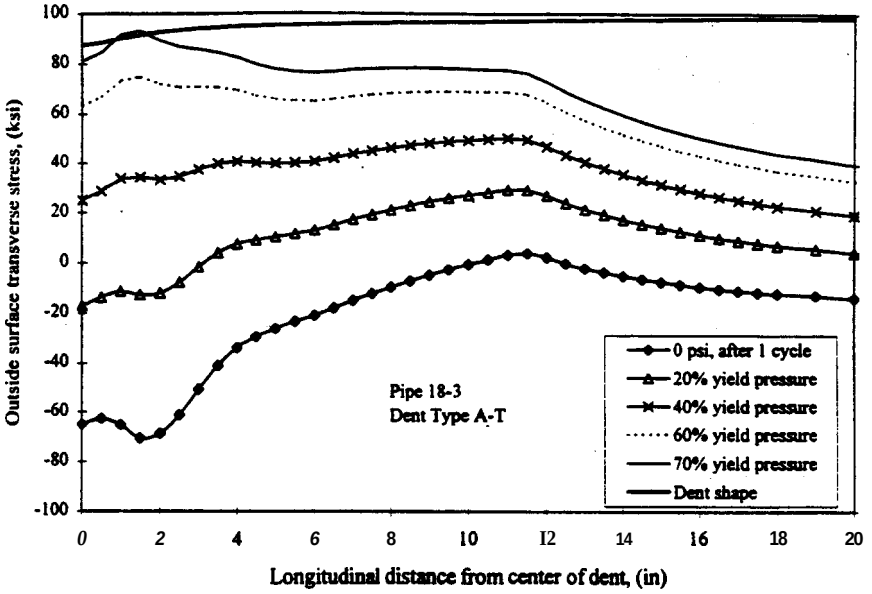

Figure 4-104: Outside surface transverse stress behavior during pressure cycling for Pipe 18-3 with a 10 percent *d/D* Type A-T dent.

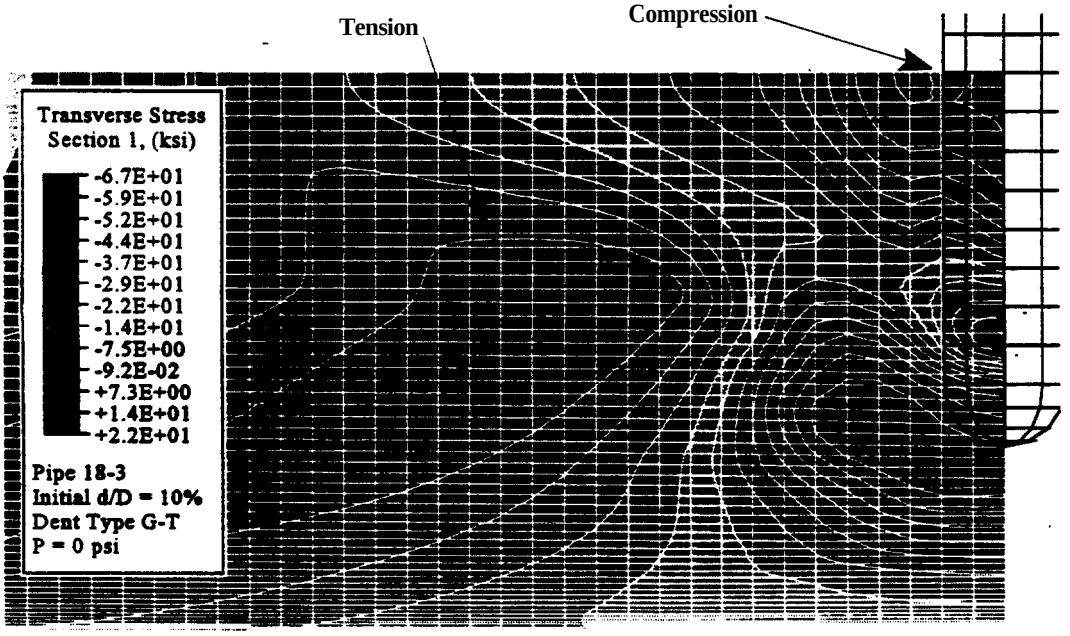

Figure 4-105: Outside Surface transverse *stress* contour plot for Pipe 18-3 with a 10 percent *d/D* Type G-T dent at 0 psi.

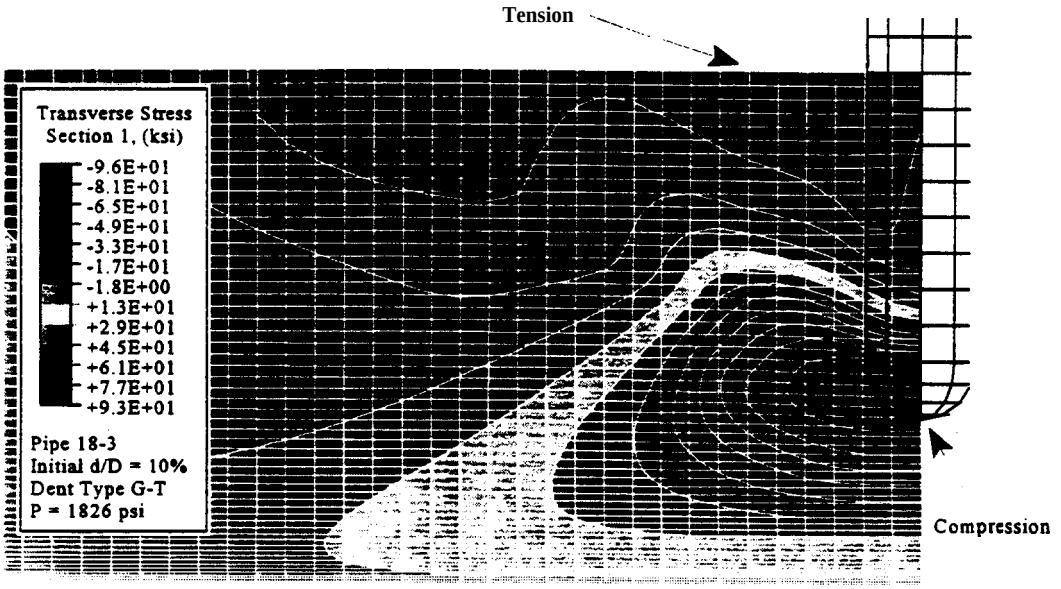

Figure 4-106: Outside surface transverse stress contour plot for Pipe 18-3 with a 10 percent *d/D* Type G-T dent at the design pressure.

The typical stress behavior of transverse dents found for the 48 in. models is given in Fig. 4-107 for a 10 percent *d/D* Type A-T dent in Pipe 48-4. Unlike the 18 in. models, the contact region does not have a high stress range for the larger diameter models. A high peripheral transverse stress range suggests longitudinal peripheral fatigue failures for large diameter pipes with transverse dents.

The longitudinal stress behavior of transverse dents may also cause fatigue crack development. The outside longitudinal stress distribution for a 10 percent *d/D* Type A-T Dent in Pipe 18-3 is given in Fig. 4-108. The contact region has a high stress range. This could lead to the formation of transverse fatigue cracks in the damaged contact region. This longitudinal stress behavior is found for all transverse dents modeled. The stress range is dependent on the initial dent depth.

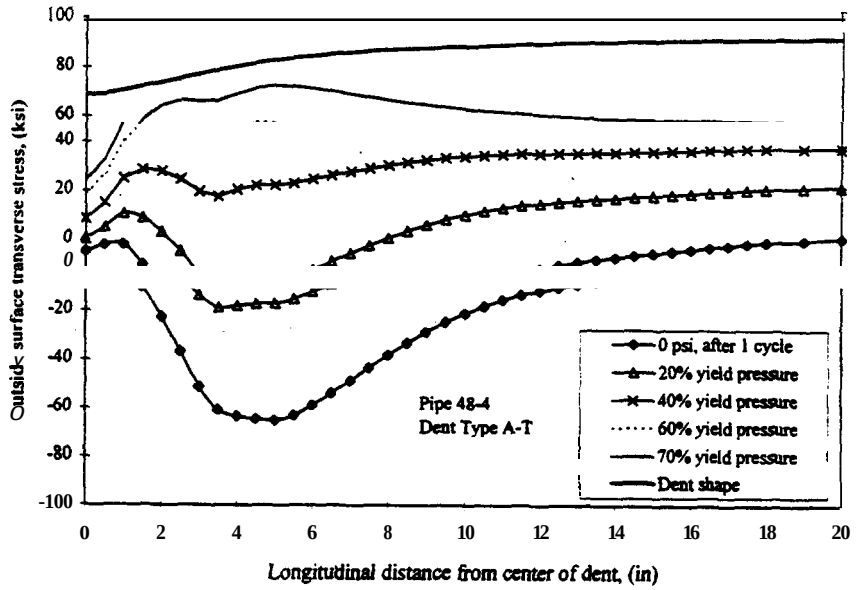

Figure 4-107: Outside surface transverse stress behavior during pressure cycling for **Pipe 48-4 with a 10 percent *d/D* Type A-T dent.**

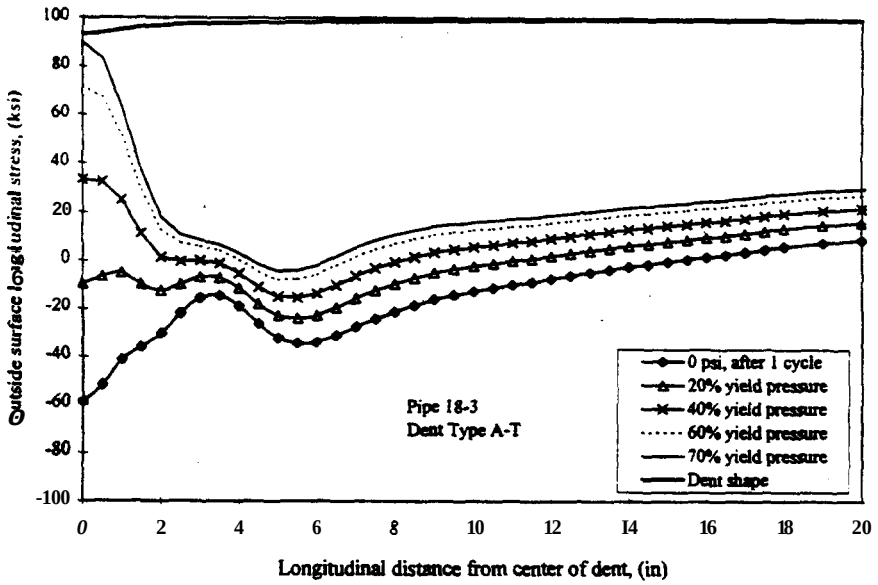

Figure 4-108: Outside surface longitudinal stress behavior during pressure cycling for Pipe 18-3 with **a 10 percent *d/D*** Type **A-T dent.**

Contour plots of the outside surface longitudinal stress for a 10 percent *d/D* Type G-T dent at 0 psi and the design pressure are given in Figs. 4-109 and 4-110, respectively. At 0 psi, the center of the contact region is in a stress state of compression. With pressurization, the contact region undergoes a stress reversal to a high state of tensile stress. As with the transverse stress, the longitudinal stress at the ends of contact maintains a compressive stress state through pressure cycling.

Transverse unrestrained dents can potentially develop longitudinal or transverse fatigue cracks based on the results of the Type A-T and G-T dents modeled for 18 in. and 48 in. diameter pipes. Additional investigation of transverse dents is needed to fully understand the behavior of transverse dents based primarily on dent length, depth, and diameter.

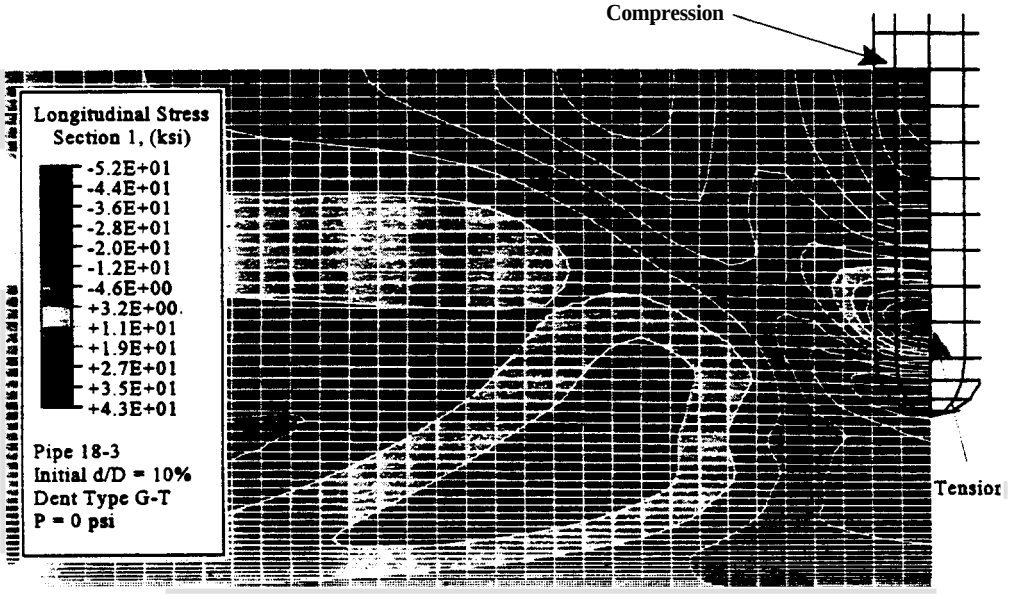

Fi 4-109: Outside surface ı; s contour plot for Pipe 18-3 with a 10 p) Type G- dent at 0 psi.

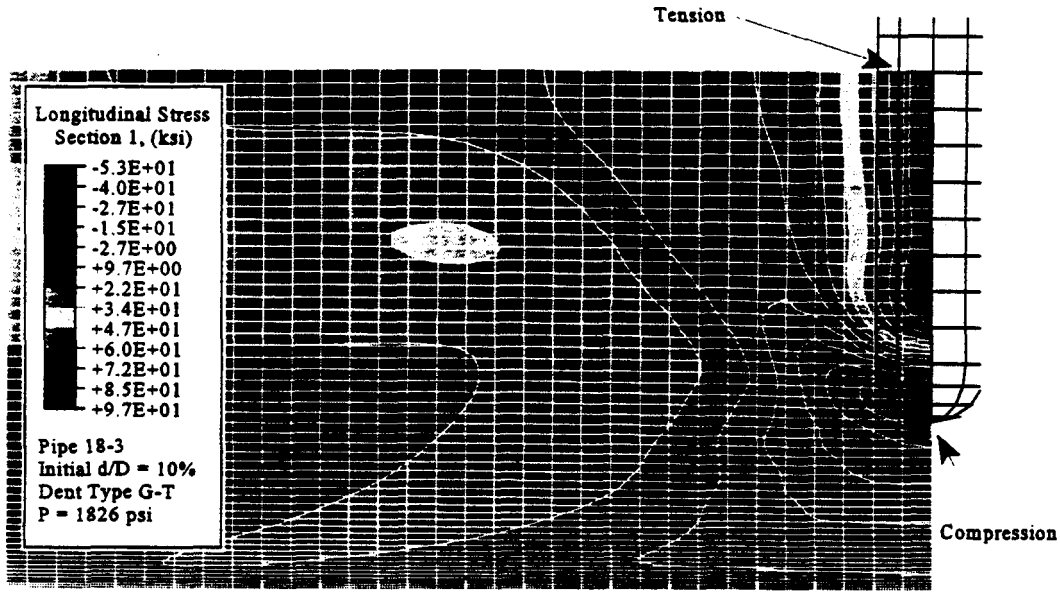

Figure 4-110: Outside surface longitudinal stress contour plot for Pipe 18-3 with a 10 percent *d/D* **Type G-T** dent at the design pressure.

4.6.2 Spherical Dents

Unrestrained spherical dents were modeled for **Type** S1 and **S8** indenters which represent 1 in. and **8** in. spheres, respectively. All other unrestrained dent **types are** cylindrical in shape resulting in a flat contact region that is relatively flexible to rebound. Spherical indenters cause the contact region to deform to the circular **shape** of the indenter. A model plot of indentation of **a** 10 percent *d/D* **Type S8** dent is given in Fig. 4-111. For comparisons with other dent types, the dented shape is similar to that of the longitudinal **Type** BH dents (Fig. **4-1**3). The contact length of **Type** BH dents is **2** in. Spherical dents have circular contact regions where the contact area is influenced by indenter diameter, dent depth, and pipe diameter. The diameter of the circular contact region for the dent in Fig. 4-111 is **over 4** in. Deeper **dents** will have larger contact areas.

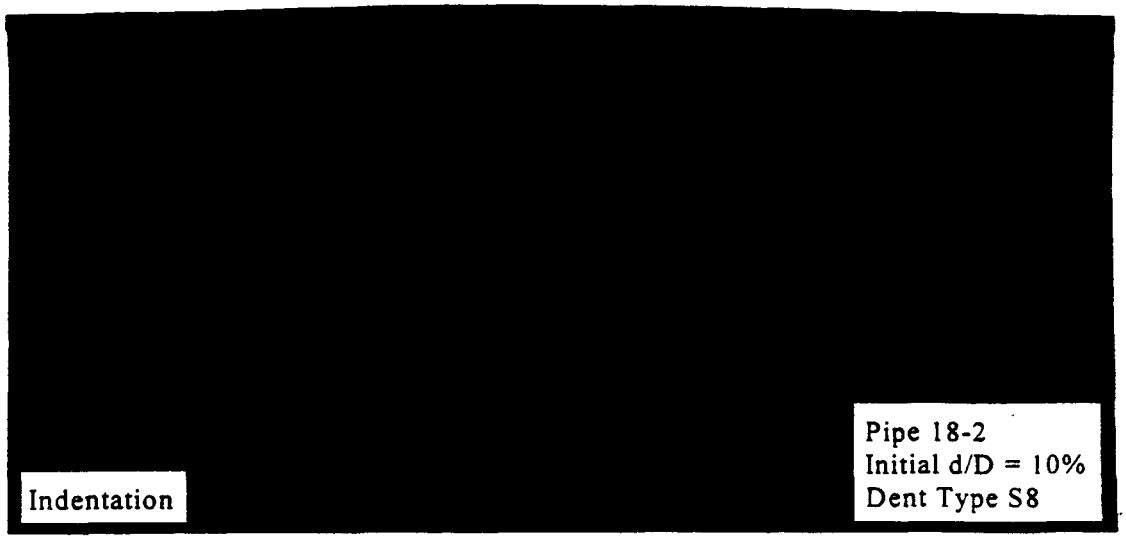

Figure **4-111:** Dent Type **S8** model plot of indentation.

The rebound characteristics of dent Types S1 and S8 *are* very similar to that of **Type** BH dents. Of the three dent **types,** Type S1 **has** the smallest contact area and the least amount of rebound. **Type** S8 **has** the largest contact area and the most amount of rebound. A graph of fmal *d/D* vs initial ***d/D*** for dent Types S1 and **S8** is given in Fig. 4-1 12 for the pipe sizes modeled. For both pipes ***sizes*** modeled, the Type **S8** dents have more rebound **than** the Type S1 dents. The dents in the large diameter models have more rebound **than** the dents in the smaller models.

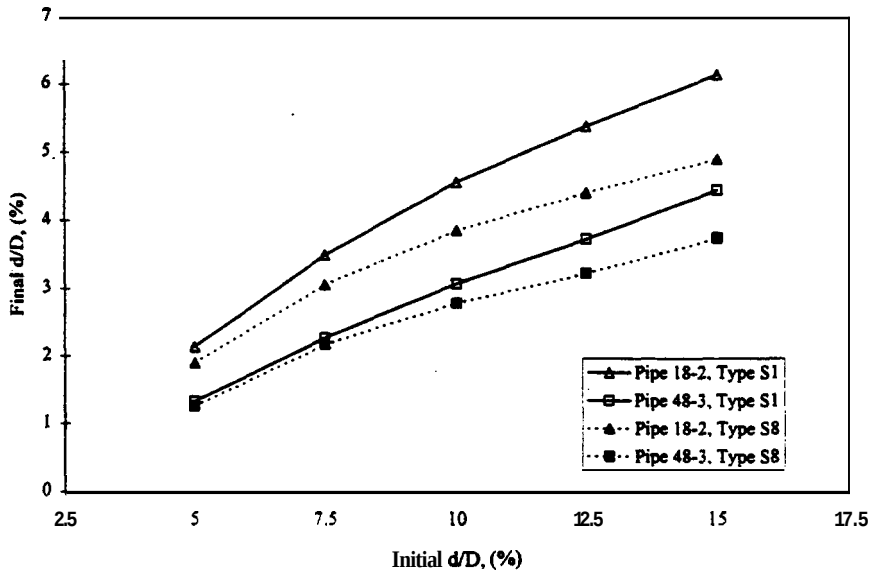

Figure 4-112: Final dent depth (*d/D*) vs. initial dent depth (*d/D*) for dent Types S1 and S8.

The averaged Rebound Ratios for the spherical unrestrained dents modeled is given in Table 4-16. From Table 4-8, the averaged Rebound Ratios for Type BH dents in Pipes 18-2 and 48-3 are 0.38 and 0.27, respectively. These values are near those given in Table 4-16 for the Type S1 and S8 dents.

Table 4-16: Rebound Ratio for spherical dents.

Thickness, t (in.)	Diameter, *D* (in.)			
	18		48	
	S1	S8	S1	S8
0.250	0.44	0.37	----	----
0.375	----	----	0.30	0.27

The stress behavior of unrestrained spherical dents is similar to the behavior of unrestrained Type BH dents. This was expected since the different dent types had similar rebound characteristics. As with Type BH dents, longitudinal peripheral fatigue cracks can develop around unrestrained spherical dents. The outside surface transverse stress distribution during pressure cycling is given in Fig. 4-113 for a 10 percent *d/D* Type S8 dent in Pipe 18-2. This stress distribution with a high peripheral stress range is typical of all unrestrained spherical dents modeled.

The circular shape of the contact region provides enough local dent stiffness to cause Mode 2 or short dent behavior. The fatigue strength of spherical dents will be similar to that of Type BH dents due to the similarities of rebound and stress behavior.

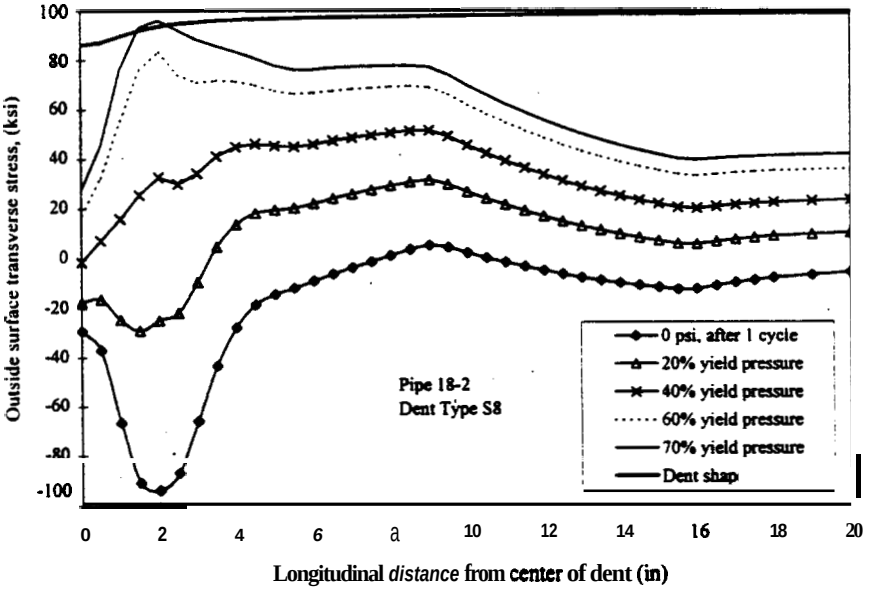

Figure 4-113: Outside surface transverse stress behavior during pressure cycling for Pipe 18-2 with a 10 percent *d/D* type S8 dent.